PHYSICAL REVIEW B **81**, 054512 (2010)

Conductivity of hard core bosons: A paradigm of a bad metal

Netanel H. Lindner and Assa Auerbach
Physics Department, Technion, Haifa 32000, Israel

(Received 28 October 2009; revised manuscript received 28 December 2009; published 18 February 2010)

Two-dimensional hard core bosons suffer strong scattering in the high-temperature resistive state at half filling. The dynamical conductivity $\sigma(\omega)$ is calculated using nonperturbative tools such as continued fractions, series expansions, and exact diagonalization. We find a large temperature range with linearly increasing resistivity and broad dynamical conductivity, signaling a breakdown of Boltzmann-Drude quasiparticle transport theory. At zero temperature, a high-frequency peak in $\sigma(\omega)$ appears above a "*Higgs mass*" gap and corresponds to order-parameter magnitude fluctuations. We discuss the apparent similarity between conductivity of hard core bosons and phenomenological characteristics of cuprates, including the universal scaling of Homes *et al.* [Nature (London) **430**, 539 (2004)].

DOI: 10.1103/PhysRevB.81.054512 PACS number(s): 05.30.Jp, 72.10.Bg, 74.72.−h, 78.67.−n

I. INTRODUCTION

Quantum transport in condensed matter is largely based on the paradigms of Fermi and Bose gases. Boltzmann equation for the conductivity is valid in the weak scattering regime where it yields a Drude form[1,2]

$$\sigma^{Drude}(T,\omega)=\frac{q^2 n}{m^*}\mathrm{Re}\frac{\tau}{1-i\omega\tau}, \tag{1}$$

where T is the temperature, ω is the frequency, and $q,n,m^*,\tau(T)$ are the charge, density, effective mass, and scattering time of the constituent quasiparticles.

Interacting bosons in a strong periodic potential may suffer strong enough scattering which invalidates Boltzmann-Drude theory. An example is provided by the two-dimensional hard core bosons (HCB) model at half filling. While it is established that the ground state is a *bona fide* superconductor,[3–7] the resistive (normal) phase involves strongly interacting bosons and vortex pairs. Previous work[8,9] showed that the lattice (umklapp) scattering dramatically increases vortex mobility. At half filling, it produces an abrupt reversal of the Hall conductivity and doublet degeneracies associated with each vortex.

HCB models may be experimentally relevant to cold atoms in optical lattices,[10,11] underdoped cuprate superconductors,[12–14] low capacitance Josephson-junction arrays,[15,16] and disordered superconducting films.[17] An added advantage of HCB is that they are described by a quantum spin-half XY model which is amenable to tools of quantum magnetism.

It is the purpose of this paper to compute the conductivity of HCB at half filling. We apply and test a set of nonperturbative approaches, including continued fraction representation, series expansions, and exact diagonalization (ED). By studying the dynamical structure of the Kubo formula, we can construct well-converging approximants which agree with high accuracy sum rules in a wide regime of temperature. The conductivity at high temperatures is obtained to order of T^{-3}. Near the superconducting transition, it is matched with the critical conductivity which was derived by Halperin and Nelson (HN).[18] At zero temperature, the dynamical conductivity is obtained from the relativistic Gross-Pitaevskii (RGP) field theory and a variational fit to 12th order moments.

Our key results pertain to the qualitative effects of strong scattering on the conductivity. At high temperatures, the conductivity goes as

$$\sigma(T,\omega)\approx 0.91\frac{q^2}{h}\frac{\tanh[\hbar\omega/(2T)]}{(\omega/\bar{\Omega})}\exp\left[-\left(\frac{\omega}{\bar{\Omega}}\right)^2\right], \tag{2}$$

where $\bar{\Omega}$ is a high-frequency scale. Eq. (2), when fit at low frequencies and temperatures, to the form (1), yields an "effective scattering rate" which is equal to $2T$. The resistivity as shown in Fig. 1 exhibits "bad metal"[19] behavior: it exceeds the boson Ioffe-Regel limit[20] of $R>h/q^2$, without saturation.[21,22] The magnitude of the T^{-3} term is relatively small, which yields a nearly T-linear resistivity from about $T=2T_{\mathrm{BKT}}$ to infinite temperature. The resistivity's linear

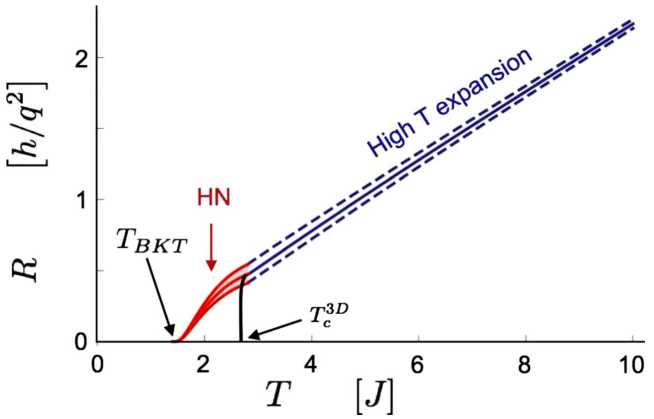

FIG. 1. (Color online) Temperature-dependent resistivity of two-dimensional hard core bosons at half filling. High-temperature line (blue online) is calculated up to order $1/T$, with error margins depicted by dashed lines. The critical region above the BKT transition is given by the vortex plasma theory of HN. For illustration, a layered system with weak interlayer coupling shows a rapid rise in resistivity above the three-dimensional transition temperature T_c^{3D}, as depicted by a solid black line.

slope defines the proportionality coefficient between the zero-temperature superfluid stiffness and product of T_c and the normal-state conductivity near T_c. We note that linearly increasing resistivity[23] and an analogous scaling of superfluid stiffness with conductivity called "Homes law"[24] have been observed in the cuprate family, as depicted in Fig. 9.

In addition, at zero temperature we find a small conductivity peak above a "Higgs mass" gap. This peak is associated with order-parameter magnitiude fluctuations. These are analogous to coherence oscillations observed in cold atoms during rapid Mott to superfluid quenches.[25–27] We speculate that perhaps the *mid infrared* peak observed in some cuprates at low temperatures[28] might arise from these magnitude fluctuations.

However we emphasize that similarities between HCB and cuprates are only suggestive. As we only study the simplest square lattice model at half filling with no extra interactions, we do not claim that these results are universal, although we expect them to by typical. In the context of cuprate superconductors, we *do not* include fermion quasiparticles, magnetic excitations, and inhomogeneities which are known to be important in the experimental systems.

This paper is organized as follows: Sec. II introduces the HCB model and lists some of the established thermodynamics. Section III discusses the Kubo formula, in general, and derives the moment expansion, continued fraction recurrents, and orthogonal polynomials which can be used to evaluate σ nonperturbatively and generate a high-temperature expansion. Section IV derives the particular recurrents for the HCB at half filling. Justification for the rapidly converging harmonic-oscillator expansion is provided. Sections III and IV are quite technical and could be avoided at first reading. The results of our calculations are provided in the following sections. Section V plots the dynamical conductivity at high temperatures and explains three approaches which converge to the same curve. Section VI obtains the resistivity as a function of temperature. Section VII obtains the dynamical conductivity and Higgs mass at zero temperature. Section VIII summarizes the key results and discusses their possible relevance to the dynamical and dc conductivity of cuprate superconductors.

II. HARD CORE BOSONS

Hard core bosons are defined on lattice sites $i=1,\ldots,N$ with restricted occupation numbers, $n_i=0,1$. The constrained creation operators $\tilde{a}_i^\dagger$ are represented by spin-half raising operator

$$\tilde{a}_i^\dagger = S_i^+ = S_i^x + iS_i^y,$$

$$\tilde{a}_i = S_i^-. \tag{3}$$

Thus, their commutation relations are

$$[S_i^-, S_j^+] = -\delta_{ij} 2S_i^z \rightsquigarrow [\tilde{a}_i, \tilde{a}_j^\dagger] \equiv \delta_{ij}(1-2n_i). \tag{4}$$

A minimal model of HCB hopping with Josephson coupling J, coupled to an electromagnetic field A_{ij}, is the gauged $S=\frac{1}{2}$ quantum XY model,

$$H = -2J\sum_{\langle i,j\rangle} (e^{iqA_{ij}}\tilde{a}_i^\dagger \tilde{a}_j + \text{H.c.}) = -2J\sum_{\langle i,j\rangle} (e^{iqA_{ij}}S_i^+ S_j^- + \text{H.c.}), \tag{5}$$

where q is the boson charge (=$2e$, for electronic superconductors) and we use units of $\hbar=c=1$. Here we consider $\langle i,j\rangle$ to be nearest-neighbor bonds on the square lattice. In the absence of a chemical potential (i.e. a Zeeman field coupled to $\Sigma_i S_i^z$), the Hamiltonian describes a density of half filling (zero magnetization), with half a boson per site.

The uniform current operator, for $\mathbf{A}=0$, is given by

$$J_x = -\frac{2iqJ}{\sqrt{N}}\sum_{\langle i,j\rangle} (\tilde{a}_i^\dagger \tilde{a}_j - \tilde{a}_j^\dagger \tilde{a}_i) = \frac{4qJ}{\sqrt{N}}\sum_{\mathbf{r}} (S_{\mathbf{r}}^x S_{\mathbf{r}+\hat{\mathbf{x}}}^y - S_{\mathbf{r}}^y S_{\mathbf{r}+\hat{\mathbf{x}}}^x). \tag{6}$$

We note that in one dimension, the current of HCB is a conserved operator since

$$[H^{1D}, J_x] = 0 \tag{7}$$

and hence the real conductivity trivially vanishes at all finite frequencies and temperatures. In two and higher dimensions, this is not the case: the conductivity has nontrivial dynamical structure. Below we review some established results for the thermodynamic properties of the two-dimensional quantum XY model which are relevant to the conductivity.

A. Superfluid stiffness

It is widely believed that at zero temperature H has long-range order. Thus, at low temperatures $T\geq 0$, the *two-dimensional boson superfluid stiffness* ρ_s, which has units of energy, is finite

$$\rho_s \equiv q^{-2} \left.\frac{d^2F(T,n)}{(dA_x)^2}\right|_{\mathbf{A}=0} > 0, \tag{8}$$

where F is the free energy in the presence of a uniform field $\mathbf{A}=A_x\hat{\mathbf{x}}$. A classical (mean-field) approximation at zero temperature yields a nonmonotonous density dependence,

$$\rho_s^{cl}(0,n) = 4Jn(1-n), \tag{9}$$

where n is the mean boson occupation (filling). Half filling $n=\frac{1}{2}$ is "*optimal*," with maximal ρ_s. Quantum corrections to $\rho_s^{cl}(0,\frac{1}{2})$ enhance it by about 7%.[6,7]

B. BKT Transition

The *static* order-parameter correlations of Eq. (5) are described by a renormalized classical XY model. At low temperatures, correlations decay as a power law in distance. $\rho_s(T)$ decreases with T, until it falls discontinuously to zero at T_{BKT}, the Berezinskii-Kosterlitz-Thouless (BKT) transition temperature.[29–31] At half filling, quantum Monte Carlo (QMC) simulations of Eq. (5) have determined,[4,5]

$$T_{\text{BKT}} \simeq 1.41J. \tag{10}$$

Just below the transition, a universal relation holds

$$\rho_s(T_{\mathrm{BKT}}) = \frac{2}{\pi} T_{\mathrm{BKT}}. \tag{11}$$

For $T > T_{\mathrm{BKT}}$, $\rho_s = 0$, and the correlation length is

$$\xi \sim A \exp\left(\frac{B}{\sqrt{(T - T_{\mathrm{BKT}})/T_{\mathrm{BKT}}}} \right), \tag{12}$$

where $A = 0.285$ and $B = 1.92$ as determined by QMC.[5]

In multilayered systems with weak interlayer coupling[14,32,33] $J_c \ll J$, the three-dimensional (3D) transition temperature is higher than T_{BKT} by a factor,

$$T_c^{\mathrm{3D}} = T_{\mathrm{BKT}} \left(1 + \frac{B^2}{\log^2(0.144 J/J_c)} \right). \tag{13}$$

C. Boson particle-hole symmetry

The charge-conjugation operator

$$C = e^{i\pi \Sigma_i S_i^x} \tag{14}$$

transforms particles into oppositely charged holes,

$$\tilde{a}_i \to \tilde{a}_i^\dagger,$$

$$n_i \to (1 - n_i),$$

$$H[q\mathbf{A}, n] \to H[-q\mathbf{A}, 1 - n]. \tag{15}$$

It follows therefore that under reflection about half filling, the Hall conductivity reverses sign while the superfluid stiffness and longitudinal conductivity are invariant.

In the low-density limit $n \ll \frac{1}{2}$, the HCB are effectively unconstrained[34,35] as seen by Eq. (4). This can be demonstrated by expanding the Holstein-Primakoff bosons representation of spin half,

$$\tilde{a}_i = b_i^\dagger \sqrt{1 - n_i^b} \approx b_i^\dagger \left[1 - \frac{1}{2} n_i^b + \mathcal{O}(n_i^b)^2 \right]. \tag{16}$$

Truncating the expansion [Eq. (16)], and inserting it into H, turns it into an interacting *soft bosons* model. At low densities, the low excitations of H do not feel the lattice. Thus, the long-wavelength properties are well described by the Galilean invariant Gross-Pitaevskii (GP) field theory[10] and the mean-field superfluid stiffness goes as

$$\rho_s \sim 4Jn \equiv \frac{\hbar^2}{m_b a^2} n, \tag{17}$$

where m_b, a are the boson effective mass and lattice constant, respectively. Similarly, by particle-hole transformation [Eq. (15)], H simplifies into a model of weakly interacting holes as $n \to 1$.

It is around half filling, however, that higher order interactions in Eq. (16) and lattice effects become relevant. The Galilean invariant (nonrelativistic) GP theory fails to account for important umklapp scattering processes which lead to Hall-effect cancellation and doublet degeneracies of vortex states.[8]

III. NONPERTURBATIVE ANALYSIS OF THE KUBO FORMULA

A. Current fluctuations function

Thermodynamic averages are denoted by

$$\langle (\cdot) \rangle_\beta = \frac{1}{Z} \mathrm{Tr}[e^{-\beta H}(\cdot)], \quad Z = \mathrm{Tr}\, e^{-\beta H}, \tag{18}$$

where $\beta = 1/T$. The linear-response Kubo formula for the longitudinal dynamical conductivity is[36]

$$\sigma(\beta, \omega) = i \frac{\langle -q^2 K_x \rangle_\beta - \Lambda_{xx}(\beta, \omega + i\epsilon)}{\omega + i\epsilon}, \tag{19}$$

where

$$K_x = -\frac{4J}{N} \sum_{\mathbf{r}} (S_{\mathbf{r}}^x S_{\mathbf{r}+\mathbf{x}}^x + S_{\mathbf{r}}^y S_{\mathbf{r}+\mathbf{x}}^y) \tag{20}$$

is the x kinetic energy and Λ is the retarded current-current response function

$$\Lambda_{xx}(z) = \int_0^\infty dt e^{izt} \langle [J_x(t), J_x(0)] \rangle_\beta$$

$$J_x(t) \equiv e^{iHt} J_x e^{-iHt}, \tag{21}$$

where the HCB current operator is given by Eq. (6).

The (real) conductivity is given by

$$\sigma(\beta, \omega) = q^2 \pi \rho_s(\beta) \delta(\omega) + \frac{\tanh(\beta\omega/2)}{\omega} G''(\beta, \omega),$$

$$G''(\beta, \omega) = \frac{1}{2} \int_{-\infty}^\infty dt e^{-i\omega t} \langle \{ J_x(t), J_x(0) \} \rangle_\beta. \tag{22}$$

where $\{\cdot, \cdot\}$ is an anticommutator.

The *current fluctuations function* $G''(\beta, \omega)$ of HCB at half filling is our primary object of attention. We cannot rely on a nearly free quasiparticle basis about which to expand Eq. (5) or Eq. (6). We therefore turn our attention to nonperturbative approaches.

B. Moments expansion

It is advantageous in our case, to analyze the dynamical structure of $G''(\omega)$ in the operator Hilbert space (OHS). The OHS is a linear space of HCB (spin-half) operators, denoted by capital roman letters, $A, B, \ldots$, which are the "hyperstates" of the OHS. In this paper, we use two different inner products.

(i) The infinite temperature product,

$$(A, B)_\infty = \frac{1}{2^N} \mathrm{Tr}(A^\dagger B). \tag{23}$$

(ii) The zero-temperature product,

$$(A, B)_0 = \langle 0 | A^\dagger B | 0 \rangle, \tag{24}$$

where $|0\rangle$ is the ground state of the Hamiltonian H. It is easy to verify that both definitions obey the Hilbert-space condi-

tions for an inner product. Henceforth, we unify the notations and drop the subscripts $0,\infty$.

"*Hyperoperators*," denoted by capital script letters, are linear operators which act on hyperstates of the OHS. The *Liouvillian* hyperoperator $\mathcal{L}$ is defined by its action on any hyperstate A as

$$\mathcal{L}A \equiv [H,A]. \tag{25}$$

By Hermiticity of H and the cyclic property of the trace, the Liouvillian $\mathcal{L}$ is Hermitian for *both* definitions of the inner products [Eqs. (23) and (24)],

$$(A,\mathcal{L}B) = (B,\mathcal{L}A)^*. \tag{26}$$

Therefore, $\mathcal{L}$ has a real eigenspectrum.

The time-dependent current operator in the Heisenberg representation $J_x(t)$ is compactly expressed using the evolution hyperoperator,

$$J_x(t) = e^{i\mathcal{L}t}J_x. \tag{27}$$

The hyper-resolvent $\mathcal{G}(z)$,

$$\mathcal{G}(z) = \frac{1}{z-\mathcal{L}}, \tag{28}$$

is related to the evolution hyperoperator by

$$e^{i\mathcal{L}t} = \oint \frac{dz}{2\pi i} e^{izt}\mathcal{G}(z). \tag{29}$$

The contour surrounds the spectrum of $\mathcal{L}$, which by Eq. (26) lies on the real axis.

The complexified current fluctuations function is

$$G(\beta,z) = \frac{1}{Z}\mathrm{Tr}(e^{-\beta H}\{J_x,\mathcal{G}(z)J_x\}). \tag{30}$$

Equation (22) is recovered by its imaginary part on the real axis,

$$G''(\beta,\omega) = -\frac{1}{Z}\mathrm{Im}\ \mathrm{Tr}\left(e^{-\beta H}\left\{J_x,\frac{1}{\omega-\mathcal{L}+i\epsilon}J_x\right\}\right). \tag{31}$$

A direct $1/\omega$ expansion of $(\omega-\mathcal{L})^{-1}$ does not yield the required imaginary function.[37] To extract G'' one uses complex analysis

$$\oint dz z^k \mathcal{G}(z) = \oint \frac{dz}{z} z^k \sum_{n=0}^{\infty}\left(\frac{\mathcal{L}}{z}\right)^n = 2\pi i \mathcal{L}^k \tag{32}$$

and take the contour around the real axis to obtain the sum rules for all $k=0,2,4,\ldots,\infty$,

$$\int_{-\infty}^{\infty}\frac{d\omega}{\pi}\omega^k G''(\beta,\omega) = \langle\{J_x,\mathcal{L}^k J_x\}\rangle_\beta \equiv \mu_k(\beta). \tag{33}$$

All odd-k moments vanish by symmetry of $G''(\omega)$. The moments μ_k are static (equal-time) correlators, which can be evaluated numerically or by series expansions. It is possible, in general, to compute only a finite number of μ_k's. The remaining task is to derive converging approximants to $G''(\beta,\omega)$ by, in a sense, inverting Eq. (33).

C. Liouvillian matrix

In order to invert Eq. (33), we use the structure of the Liouvillian matrix. A tridiagonal matrix representation of the Liouvillian is constructed as follows. We define the root hyperstate by the current operator,

$$\hat{O}_0 = \frac{1}{\sqrt{(J_x,J_x)}}J_x. \tag{34}$$

An orthonormal set of hyperstates $\hat{O}_n$ can be generated by sequentially applying $\mathcal{L}$ and orthonormalizing by the Gram-Schmidt procedure,

$$\hat{O}_{n+1} \equiv c_{n+1}(\mathcal{L}\hat{O}_n - \Delta_n\hat{O}_{n-1}), \quad n=1,2,\ldots,$$

$$\Delta_n = (\hat{O}_{n-1},\mathcal{L}\hat{O}_n),$$

$$c_{n+1} = [(\hat{O}_n,\mathcal{L}^2\hat{O}_n) - |\Delta_n|^2]^{-1/2}, \tag{35}$$

where $\Delta_0=0$. Since J_x is Hermitian and $\mathcal{L}J_x$ is anti-Hermitian, all $\hat{O}_n$ can be chosen to be Hermitian (anti-Hermitian) for even (odd) n since Δ_n will be real. Thus it is easy to prove, for both inner products defined in Eqs. (23) and (24), that $\mathcal{L}$ has no diagonal matrix elements $(\hat{O}_n,\mathcal{L}\hat{O}_n)=0$. Also, it is straightforward to prove by induction that $|\hat{O}_n\rangle$ is an orthonormal set,

$$(\hat{O}_n,\hat{O}_{n'}) = \delta_{nn'}, \quad n,n'=0,1,\ldots,\infty. \tag{36}$$

In this basis, $\mathcal{L}$ is given by the *Liouvillian matrix*,

$$L_{nn'} \equiv \langle\hat{O}_n|\mathcal{L}|\hat{O}_{n'}\rangle = \begin{pmatrix} 0 & \Delta_1 & 0 & 0 \\ \Delta_1^* & 0 & \Delta_2 & 0 \\ 0 & \Delta_2^* & 0 & \Delta_3 \\ 0 & 0 & \Delta_3^* & \cdots \end{pmatrix}. \tag{37}$$

In both $T=0,\infty$ limits, the current fluctuations function [Eq. (30)] is given by the root expectation value of the resolvent,

$$G(z) = (J_x,(z-\mathcal{L})^{-1}J_x) = \mu_0(z-L)^{-1}_{00}, \tag{38}$$

where $\mu_0=(J_x,J_x)$ is the corresponding zeroth moment.

In these limits, all moments of Eq. (33) are root expectation values,

$$\mu_k = (J_x,\mathcal{L}^k J_x). \tag{39}$$

Using Eq. (37), an explicit and useful relation between recurrents and moments is obtained

$$\mu_k[\Delta] = \mu_0(L^k)_{00},$$

$$\mu_2/\mu_0 = |\Delta_1|^2,$$

$$\mu_4/\mu_0 = |\Delta_1|^4 + |\Delta_1|^2|\Delta_2|^2,$$

$$\mu_6/\mu_0 = |\Delta_1|^6 + 2|\Delta_1|^4|\Delta_2|^2 + |\Delta_1|^2|\Delta_2|^4 + |\Delta_1|^2|\Delta_2|^2|\Delta_3|^2,$$

$$\vdots = . \tag{40}$$

D. Continued fraction representation

Inverting $z-L$ in Eq. (38) using elementary algebra yields the continued fraction representation[38,39]

$$G(z) = \mu_0 \frac{1}{z - \dfrac{|\Delta_1|^2}{z - \dfrac{|\Delta_2|^2}{z - \cdots}}}. \tag{41}$$

At zero temperature we obtain

$$G_{T=0}(z) = 2\langle 0|J_x^2|0\rangle \frac{1}{z - \dfrac{|\Delta_1^0|^2}{z - \dfrac{|\Delta_2^0|^2}{z - \cdots}}}, \tag{42}$$

where $|0\rangle$ is the ground state of H. Similarly, in the high-temperature limit, the leading order $G(z)$ is given by

$$G_{T=\infty}(z) = \frac{2}{2^N}\mathrm{Tr}(J_x^2) \frac{1}{z - \dfrac{|\Delta_1^\infty|^2}{z - \dfrac{|\Delta_2^\infty|^2}{z - \cdots}}}. \tag{43}$$

The infinite list of recurrents fully determines $G''(\omega)$. If only a finite set is computable, extrapolation of $|\Delta_n|^2$ to large n is unavoidable. Some intuition about the relation between recurrents and the imaginary part of the continued fraction function at $z \to \omega + i\epsilon$ is gained by the following examples, for complex functions $F(z)$, where $F(\omega+i\epsilon)=F'(\omega) - iF''(\omega)$.

(i) A Lorentzian, as given by the Drude form (1), is a *somewhat pathological limit*. All its even moments except μ_0 are infinite. This form amounts to replacing the denominator's self-energy by a purely imaginary constant,

$$F(z) = \frac{1}{z - \Sigma_1(z)},$$

$$\Sigma_1(z) = \frac{|\Delta_1|^2}{z - \dfrac{\Delta_2^2}{z - \dfrac{\Delta_3^2}{z - \cdots}}} \Rightarrow \frac{i}{\tau}. \tag{44}$$

(ii) Constant recurrents, $\Delta_n=\Delta$, $n=1,2,\ldots$, yield a semicircle imaginary part,

$$F(z) = \frac{1}{z - \dfrac{\Delta^2}{z - \dfrac{\Delta^2}{z - \cdots}}},$$

$$F''(\omega) = \sqrt{1 - (\omega/2\Delta)^2}. \tag{45}$$

(iii) Linearly increasing recurrents, $|\Delta_n|^2=n\Omega^2/2$ define the continued fractions

$$F(z) = \frac{1}{z - \dfrac{\frac{1}{2}\Omega^2}{z - \dfrac{\Omega^2}{z - \cdots}}}, \tag{46}$$

which is relevant to HCB at high temperatures, as argued in Sec. IV A In Appendix B it is shown that Im F is a Gaussian,

$$F''(\omega) = \sqrt{\frac{\pi}{\Omega^2}} \exp\left(-\frac{\omega^2}{\Omega^2}\right). \tag{47}$$

Incidentally, the real part of $F(\omega)$ is the Dawson function[40]

$$F'(\omega) = \frac{2}{\Omega}\int_0^{\omega/\Omega} e^{t^2} dt. \tag{48}$$

E. Finite temperature corrections

At finite temperatures, the current fluctuations function includes the effects of the thermal density matrix

$$\rho(\beta) = 2^N e^{-\beta H}/Z(\beta). \tag{49}$$

(The prefactor of 2^N is introduced for later convenience.) One can write

$$G(\beta,z) = (\{\rho,J_x\},\mathcal{G}(z)J_x)_\infty = \sum_n C_n(\beta)G_n(z),$$

$$C_n(\beta) = \mu_0(\{\rho(\beta),\hat{O}_0\},\hat{O}_n)_\infty,$$

$$G_n(z) = \mu_0(z-L)^{-1}_{n,0}. \tag{50}$$

Taking $z \to \omega + i\epsilon$ yields an orthogonal polynomial expansion for the current fluctuations function,

$$G''(\beta,\omega) = \sum_{n=0}^{\infty} C_n(\beta)P_n(\omega)G_0(\omega). \tag{51}$$

The polynomials P_n are orthogonal under the measure defined by $G_0(\omega)$,

$$\int_\infty^\infty d\omega P_n(\omega)P_m(\omega)G_0(\omega) = \delta_{n,m}. \tag{52}$$

In Appendix A we derive explicit expressions for P_n as a function of G_0 and the preceding recurrents $|\Delta_m|^2$, $m=1,2,\ldots,n$.

IV. KUBO FORMULA FOR HCB AT HALF FILLING

In the previous section we introduced the moments and recurrents of the current fluctuations function $G(z)$. Henceforth, we specialize to HCB at half filling. First we analyze the expected asymptotic behavior of the Liouvillian matrix elements. Second, we construct a variational harmonic-oscillator (VHO) basis in which the current fluctuations can be expanded. Third, we generate a high-temperature expansion of $G''(\beta,\omega)$.

A. Liouvillian of HCB and Gaussian asymptotics

The Liouvillian hyperoperator $\mathcal{L}$ [Eq. (25)] describes strong scattering in the following sense: when $\mathcal{L}$ acts on a hyperstate composed of n spins,

$$A_n = \sum c^{\alpha_1,\alpha_2,\ldots,\alpha_n}_{i_1,i_2,\ldots,i_n} S^{\alpha_1}_{i_1} S^{\alpha_2}_{i_2}, \ldots, S^{\alpha_n}_{i_n},$$

the number of spins increases or decreases by precisely one, i.e.,

$$\mathcal{L}A_n = A_{n+1} + A_{n-1}. \tag{53}$$

When $|A_{n+1}| \gg |A_{n-1}|$, the primary effect of $\mathcal{L}$ is to *proliferate* the number of spins.

Let us compare the behavior of HCB with weakly interacting bosons. Consider a typical boson liquid Hamiltonian

$$H^{weak} = a^\dagger H_0 a + \tfrac{1}{2} g a^\dagger a a^\dagger a. \tag{54}$$

The action of the respective Liouvillian on a linear operator yields

$$[H^{weak}, a^\dagger] = a^\dagger H_0 + g a^\dagger a a^\dagger. \tag{55}$$

Thus, when g is "smaller" than H_0, the primary effect of $\mathcal{L}$ is the first term, which *propagates* $a^\dagger$, rather than the second term which *proliferates* it.

The root hyperstate $\hat{O}_0 \propto J_x$, is bilinear in spins. By repetitive applications of $\mathcal{L}^n \hat{O}_0$ one obtains clusters of up to n spins. Consider a lattice in two dimensions or higher,[41] with coordination number $z > 2$. For a typical A_n, there are nz_{eff} available bonds to attach an extra spin to an existing cluster, where $z_{\text{eff}} < z$. Therefore, the number of distinct terms in the resulting A_{n+1} is roughly a factor of nz_{eff} more than the number of terms in A_n. We thus expect, for such a lattice, most of the weight of the hyperstate $\hat{O}_n$ to consist of n spin operators.

Since $\hat{O}_n, \hat{O}_{n-1}$ are normalized, we can crudely estimate the asymptotic n dependence of the recurrents

$$|\Delta_n|^2 \approx (\hat{O}_n, \mathcal{L}\hat{O}_{n-1})^2 \sim (4J)^2 z_{\text{eff}} n, \quad n \gg 1. \tag{56}$$

[The factor $4J$ stems from the commutation relations $[S_\alpha, S_\beta] = i\epsilon_{\alpha\beta\gamma} S_\gamma$ and the definition of Hamiltonian (5)]. As we have seen in Eq. (47), if the asymptotic relation in Eq. (56) were precise, the continued fraction expansion for G'' would lead to a perfect Gaussian of width $4\sqrt{2z_{\text{eff}}}J$. However, as demonstrated in Fig. 3 the linearity of $|\Delta_n|^2$ is *not precise*: When $\mathcal{L}$ acts on $\hat{O}_n$ it generates some small fraction of $n-1$ spin operators, which *are not included* in the term $\Delta_n \hat{O}_{n-1}$ of Eq. (35). This spoils the exact relation between the index n and the number of spin operators.

Nevertheless, the coefficients $C_n(\beta)$ in Eq. (51) are expected to converge rapidly at high temperature. Expanding $C_n(\beta)$ in a high-temperature series,

$$C_n(\beta) = \sum_i C_n^{(i)} \beta^i, \tag{57}$$

it can be verified that the contribution of any m-spin operator A_m to order β^i depends on traces such as

$$\mathrm{Tr}[\{H^i, J_x\} A_m] = 0, \quad m > i + 2. \tag{58}$$

Therefore, $C_n^{(i)}$ measures the relative weight of $i+2$ spins operators or less in $\hat{O}_n$. Since, as argued previously, these weights become smaller for large n, we can expect for fixed i that

$$\lim_{n \gg i} C_n^{(i)} \to 0. \tag{59}$$

Thus at a finite order β^i, only a finite number of $C_n^{(i)}$'s are of substantial magnitude.

Phrased differently: in an idealized situation in which $\hat{O}_n$ would contain only products of $(n+2)$ spins, the C_n's would decay with β as

$$C_n = \frac{1}{Z}\mathrm{Tr}(e^{-\beta H}\{\hat{O}_n, \hat{O}_0\}) \sim \beta^n C_n^{(n)} + O(\beta^{n+2}). \tag{60}$$

This discussion raises an obvious question: *Is there a lattice where Eq. (60) becomes precise*? We have preliminary expectations[42] that this would be the case, at least for low orders in n, for the Bethe lattice in the limit of large coordination number. The rapid convergence of the harmonic-oscillator basis discussed below indicates that the square lattice at high temperatures is not "far" from the infinite-dimensional limit.

B. Variational harmonic-oscillator expansion

A high-temperature expansion for the conductivity can be generated by choosing a convenient basis to expand $G''(\omega)$. The linear increase in the recurrents, suggested earlier in Eq. (56), implies a Gaussian decay of $G''(\omega)$ at high frequencies. Therefore it is natural to choose a VHO basis such that

$$\tilde{G}''(\beta, \omega) = \sum_{n=0} D_n(\beta) \tilde{H}_n(\omega) \psi_0^2(\omega), \tag{61}$$

where $\tilde{H}_n(\omega) = H_n(\omega/\Omega_v)/\sqrt{2^n n!}$ and

$$\psi_0^2(\omega) = \frac{1}{\sqrt{\pi \Omega_v^2}} \exp\left(-\frac{\omega^2}{\Omega_v^2}\right). \tag{62}$$

The function $\psi_0^2(\omega)$ is the VHO ground-state probability density, with a variational frequency scale Ω_v, and $\tilde{H}_n(\omega)$ are the corresponding (normalized) Hermite polynomials, which constitute an orthogonal set under the measure of $\psi_0^2(\omega)$.

The moments of $\tilde{H}_n(\omega)\psi_0(\omega)^2$ are

$$\lambda_n^k = \int_{-\infty}^{\infty} \frac{d\omega}{\pi} \omega^k \tilde{H}_n(\omega/\Omega_v) \psi_0^2(\omega)$$
$$= \pi^{-3/4} \sqrt{\frac{2^n}{n!}} (\Omega_v)^k \frac{(k/2)!}{[(k-n)/2]!} \Gamma[(k+1)/2], \tag{63}$$

for $k \geq n$. By construction, all λ_n^k vanish for $n > k$.

Using the high-temperature expansion of a finite number of moments

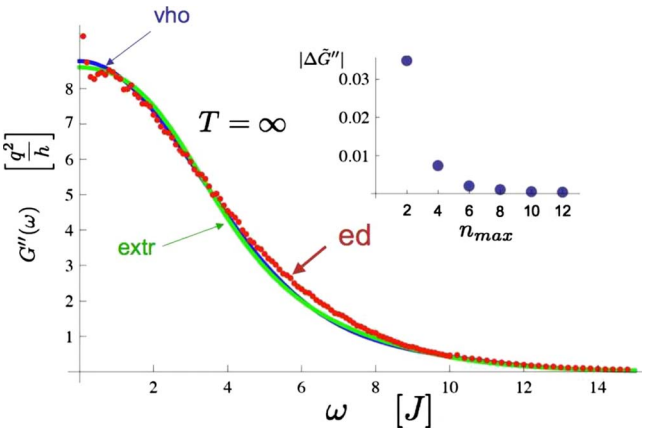

FIG. 2. (Color online) Infinite temperature current fluctuations function $G''_\infty(\omega)$. Solid lines (blue online, indicated by vho) depict the results of the variational harmonic-oscillator expansion and (green online, indicated by extr) depicts the result of the recurrents extrpolation, shown in Fig. 3. Circles (red online, indicated by ed) depict the exact diagonalization result computed on a 4×4 lattice. Inset: convergence of the variational harmonic-oscillator expansion. $|\Delta\tilde{G}''|$ are the distances between consecutive approximants and n_{max} is the number of computed moments.

$$\mu_k(\beta)=\sum_{i=0}^{\infty}\mu_k^{(i)}\beta^i,\quad k=0,2,\ldots,n_{max} \tag{64}$$

and similarly,

$$D_n(\beta)=\sum_i D_n^{(i)}\beta^i,\quad n\le n_{max}. \tag{65}$$

We insert Eq. (61) into Eq. (33) and obtain a finite set of linear equations for each $D_n^{(i)}$,

$$\sum_{n=0}^{n_{max}}\lambda_n^k D_n^{(i)}=\mu_k^{(i)}(\beta),\quad k=0,2,\ldots,n_{max}. \tag{66}$$

Solving for Eq. (66) yields the desired coefficients for Eq. (61).

V. DYNAMICAL CONDUCTIVITY: HIGH TEMPERATURE

The dynamical conductivity, to leading order in β, is

$$\sigma_{\beta\to0}=\frac{\beta}{2}G''_\infty(\omega). \tag{67}$$

We have calculated the infinite temperature current fluctuation $\tilde{G}''_{T=\infty}$, using three distinct methods. The results of the three approaches show satisfactory agreement, as depicted in Fig. 2. First we computed the infinite temperature moments, listed in Table I,

$$\mu_k^\infty=\frac{2}{2^N}\mathrm{Tr}(J_x\mathcal{L}^kJ_x),\quad k=0,2,\ldots,12. \tag{68}$$

These traces were computed numerically on a finite 16-site square lattice with periodic boundary conditions. At $k\ge8$ the calculation introduces finite-size errors due to loops of operators which circulate around the system. We eliminated most of the contributions of these loops by averaging over Aharonov-Bohm fluxes through two holes of the torus.[8]

TABLE I. Low-order moments at $T=\infty$.

k	μ_k^∞
0	4
2	64
4	4096
6	544768
8	1.20906×10^8
10	3.96113×10^{10}
12	1.75571×10^{13}

The VHO calculation of G'' follows Sec. IV B. Inverting Eq. (66), for the n_{max} lowest moments, we obtain $\tilde{G}''_{n_{max}}$. We obtain the variational frequency

$$\Omega_v=7.48J, \tag{69}$$

which minimizes the distance between the two highest order approximants,

$$|\Delta\tilde{G}''|^2(\Omega_v)=\frac{\int_{-\infty}^{\infty}d\omega|\tilde{G}''_{n_{max}}-\tilde{G}''_{n_{max}-2}|^2}{\int_{-\infty}^{\infty}d\omega|\tilde{G}''_{n_{max}-2}|^2}. \tag{70}$$

We plot $\tilde{G}''$ for $n_{max}=12$ as the solid (blue online, indicated by vho) curve in Fig. 2. In the inset of Fig. 2, we plot the convergence as a function of n_{max}. The rapid decay of $\Delta\tilde{G}''$ indicates convergence of the VHO expansion at $T=\infty$.

The second calculation extrapolates the recurrents, as shown in Fig. 3. We compute $|\Delta_n^\infty|^2$, $n=0,1,\ldots,6$, from the known moments, using Eq. (40). The higher order recurrents exhibit an approximate linear increase with $n-1$ which is consistent with a Gaussian decay of G'' at high frequencies as given by the continued fraction example of Eq. (47). We continue the linear slope (see dashed line in Fig. 3) by the extrapolation,

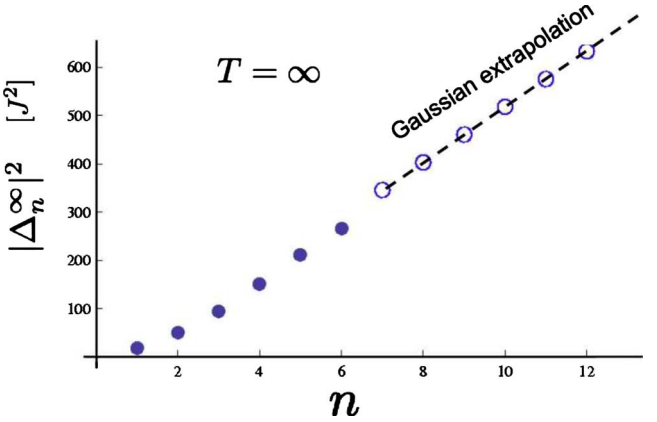

FIG. 3. (Color online) The recurrents of $G''_\infty(\omega)$ at infinite temperature and their extrapolation to large index n.

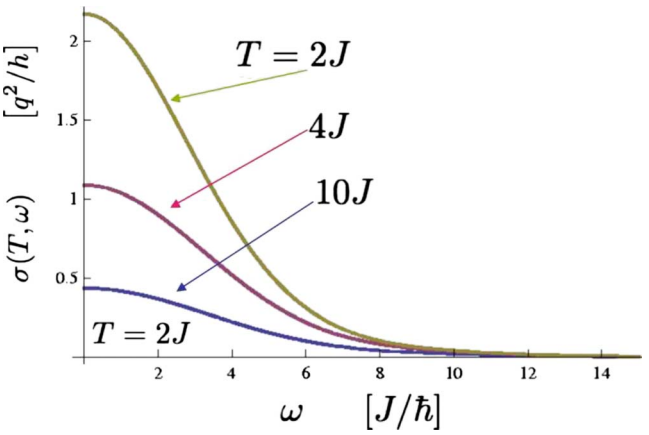

FIG. 4. (Color online) Dynamical conductivity in the high-temperature resistive phase. The function can be fit by Eq. (73).

$$|\Delta^{\infty}_{n>6}|^2 \to z_{\rm eff}(4J)^2(n-1), \quad z_{\rm eff} = 3.59, \tag{71}$$

where z_{eff} is the "effective coordination number." The approximate function $\tilde{G}''_{extr}$ is obtained using the continued fraction representation [Eq. (43)] and plotted as the solid (green online, indicated by extr) curve in Fig. 2. We notice that the two approaches yield very similar curves.

Last, we compute the infinite temperature current fluctuations function by ED in the Lehmann representation,

$$\tilde{G}''_{ed}(\omega) = \frac{2\pi}{2^N}\sum_{n,m} |\langle n|J_x|m\rangle|^2 \delta(\omega + E_n - E_m), \tag{72}$$

where $|n\rangle, E_n$ are the eigenstates and eigenspectrum of H on a 4×4 lattice with periodic boundary conditions. We expect the finite-size effects to be small at infinite temperatures, where the correlation length is much shorter than the lattice size. Indeed, the agreement between the three approaches shown in Fig. 2 supports this expectation.

Finite temperature corrections and f-sum rule

Order β^2 corrections to G'' are obtained by a high-temperature expansion of the moments $\mu^{(2)}_k$ as defined in Eq. (64). Inverting Eq. (66), the coefficients $D^{(2)}_n$ were computed up to order $n_{max}=12$ and inserted into Eq. (65). The resulting temperature-dependent dynamical conductivity is plotted in Fig. 4 for several temperatures. A crude analytical approximation is given by

$$\sigma(T,\omega) \approx 0.91\frac{q^2}{h}\frac{\tanh[\omega/(2T)]}{(\omega/\bar{\Omega})}e^{-(\omega/\bar{\Omega})^2},$$

$$\bar{\Omega} = 4.8J. \tag{73}$$

The truncation errors in the VHO expansion, and the high-temperature series, are monitored by comparing the integrated conductivity to the kinetic energy, using the f-sum-rule equation

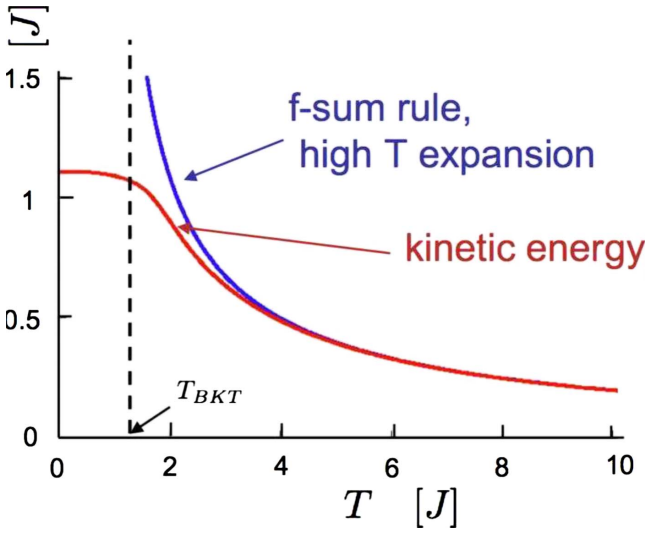

FIG. 5. (Color online) The temperature-dependent kinetic energy $\langle -K_x\rangle$ (solid, red online), calculated by Refs. 5, 6, and 43 and the sum rule for the high-temperature expansion of the dynamical conductivity of Fig. 4 (solid, blue online). The vertical dashed line marks the superconducting phase below $T_{\rm BKT}$.

$$\int_{-\infty}^{\infty}\frac{d\omega}{\pi}\frac{\tanh(\beta\omega/2)}{\omega}G''(\beta,\omega) = \langle -q^2K_x\rangle_\beta. \tag{74}$$

The values of $\langle K_x\rangle_\beta$ were computed by high-temperature series expansion up to 11th order in Ref. 43 and at low temperatures by quantum Monte Carlo simulations.[5,6] In Fig. 5 we plot the f-sum rule, Eq. (74), with G'' calculated to order β^2, and the temperature-dependent kinetic energy. The corrections grow larger than 10% at $T<2T_{\rm BKT}$.

We note, however, that numerical satisfaction of Eq. (74) does not, in general, ensure the accuracy of the dc conductivity $\sigma(0)$. In fact, there is an expectation of a cusp at zero frequency arising from high-order nonlinear coupling between the current and other long-lived diffusive modes.[44] The magnitude of this feature is expected to be weak because of particle-hole symmetry. From our calculations we can conclude that it is below the resolution provided by the exact diagonalization and the 12th order moment expansion.[45]

VI. dc RESISTIVITY: HIGH TEMPERATURE

Based on the calculations of $\sigma(T,\omega)$ of the previous section, the high-temperature expansion of the dc resistivity, shown in Fig. 1, is given to order $1/T$ as

$$R(T) = 0.23R_Q\frac{T}{J}\{1 - 2.9(J/T)^2 + \mathcal{O}[(J/T)^4]\}, \tag{75}$$

where $R_Q=h/q^2$ is the boson quantum of resistance. In the regime of $T\geq 2T_{\rm BKT}$, the negative corrections of order T^{-3} are relatively small, as the sum rule shows in Fig. 5.

As $T_{\rm BKT}$ is approached from above the resistivity drops rapidly. The critical regime was described by HN (Refs. 18, 46, and 47) who considered the contribution of unbound vortices to the charge transport coefficients. Using vortex-charge

duality and Einstein's relation for vortex conductivity, HN derived the critical resistivity as

$$R^{\mathrm{HN}} = R_Q \frac{h n_v D_v}{T}, \tag{76}$$

where D_v is the vortex diffusion constant and n_v is the density of free vortices. Estimating that $n_v = \xi(T)^{-2}$ using Eq. (12), the critical resistivity is expected to be suppressed toward T_{BKT} as

$$R^{\mathrm{HN}}(T) = R_Q \frac{h D_v n_0}{T} A^{-2} \exp\left[-2B \left(\frac{T_{\mathrm{BKT}}}{T - T_{\mathrm{BKT}}} \right)^{1/2} \right], \tag{77}$$

where n_0 is a microscopic density of order a^{-2}.

The precise diffusion constant for the HCB model is not known and can be expressed as

$$D_v n_0 = \kappa J/\hbar, \tag{78}$$

where κ is an undetermined dimensionless constant. We can estimate the numerical value of κ by requiring that $R^{\mathrm{HN}}(T)$ matches Eq. (75) at $T \geq 2T_{\mathrm{BKT}}$ where the f-sum rule is satisfied to a higher accuracy. We find that matching occurs in the range,

$$0.38 < \kappa < 0.51. \tag{79}$$

We can interpret the vortex diffusion constant $D_v = l^2/\tau$, as arising from a scattering time of order $\tau = \hbar/J$ (the intersite vortex hopping time, according to calculations of Ref. 8) and a short mean-free path $l \approx a$. Eqs. (78) and (79) are consistent with the value $D_v \approx \hbar/m$ which was posited[46] for helium films.

VII. DYNAMICAL CONDUCTIVITY: ZERO TEMPERATURE

At $T=0$ the conductivity is given by

$$\sigma_0(\omega) = q^2 \pi \rho_s \delta(\omega) + \frac{G''_{T=0}(\omega)}{|\omega|}. \tag{80}$$

We calculate the current fluctuations $\tilde{G}''_{T=0}$ in two stages. First, we appeal to the relativistic Gross-Pitaevskii field theory[48] and obtain the low-frequency gap and threshold form of the function. The mass parameter m and the high-frequency Gaussian scale Ω_0 are variational fitting parameters. Second, we compute the lowest 12 moments by exact diagonalization of a 20-site cluster. These determine the lowest recurrent parameters $|\Delta_n^0|^2$ which are fit to the variational form.

A. Field theoretical calculation

The RGP model describes the long-wavelength theory of quantum rotators in the absence of a linear time derivative term.[48] We use it to describe the HCB action at half filling, which exhibits particle-hole symmetry. $\Psi(\mathbf{r},\tau)$ denotes the fluctuating condensate order parameter, governed by the imaginary time action,

$$S_{\mathrm{RGP}} = \int d^2x \int d\tau \frac{1}{2} |\dot{\Psi}|^2 + \frac{\rho_s}{2\Delta^2} |\nabla \Psi|^2 - \frac{m}{8\Delta^2} (|\Psi|^2 - \Delta^2)^2, \tag{81}$$

where Δ is the ground-state order parameter and m is the effective (Higgs) mass. Expanding Eq. (81) to second order about $\Psi = \Delta(1+\eta)e^{i\phi}$, the harmonic fluctuations are described by decoupled phase and magnitude modes,

$$S^{(2)}_{\mathrm{RGP}} = \frac{1}{2} \int d^2x \int d\tau (\dot{\phi}^2 \Delta^2 + \rho_s |\nabla \phi|^2) + \frac{1}{2} \int d^2x \int d\tau \Delta^2 \left(\dot{\eta}^2 + \frac{\rho_s}{\Delta^2} |\nabla \eta|^2 + m \eta^2 \right). \tag{82}$$

We introduce a vector potential by shifting $\nabla \to \nabla + iq\mathbf{A}$. The current operator is obtained from $J_x = \delta S / \delta A_x$, therefore its paramagnetic part, expanded to the same order as Eq. (82), is given by

$$J_x(\mathbf{x}) = q \rho_s (\nabla \phi + 2 \eta \nabla \phi). \tag{83}$$

The lowest-order current fluctuations function is given by the bubble diagram[49,50] depicted in Fig. 6,

$$G_{\mathrm{RGP}}(i\omega_n) \simeq \frac{4q^2}{\beta} \int \sum_{\nu_n} \frac{d^2\mathbf{k}}{(2\pi)^2} \times \frac{k_x^2}{[c_s^{-2}(\omega_n + \nu_n)^2 + (\mathbf{q}+\mathbf{k})^2 + c_s^{-2} m^2][c_s^{-2} \nu_n^2 + \mathbf{k}^2)}, \tag{84}$$

where $c_s = \sqrt{\rho_s/\Delta^2}$ is the speed of sound. We compute the integral by performing the Matsubara sum, and take $\mathbf{q} \to 0$ and $\beta \to \infty$, which yields

$$G''_{\mathrm{RGP}}(\omega) \simeq \frac{q^2}{4} \left(\frac{\omega^2 - m^2}{2\omega} \right)^2 \frac{1}{|\omega|} \Theta(|\omega| - m). \tag{85}$$

The dynamical conductivity therefore exhibits finite frequency weight above the mass gap m. We cannot rule out that higher order interactions may produce subgap spectral weight since magnitude excitations can decay into phason pairs.[27]

In addition, the RGP theory Eq. (81) only describes long wave length fluctuations. Therefore, lattice scale and high-energy cutoff effects are important for the high-frequency tails of G''. These will be computed directly from the zero-temperature Kubo formula.

B. Variational fit of recurrents

The moments of $G''_{T=0}$, Eq. (33), are equal to the ground-state expectation values,

$$\mu_k = \langle 0 | \{ J_x, \mathcal{L}^k J_x \} | 0 \rangle. \tag{86}$$

We compute a set of $\mu_k, k \leq 12$ by exact diagonalizations on a 5×4 lattice. Using Eq. (40)we determine the set of recurrents $|\Delta_n|^2$, $n = 1, 2, \ldots, 6$, which are depicted in Fig. 7.

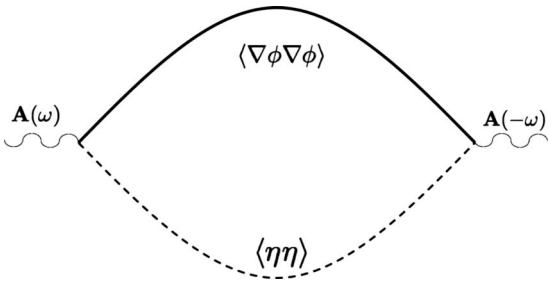

FIG. 6. Low-order current fluctuations function in the relativistic Gross-Pitaevskii field theory, as calculated by Eq. (84). Dashed line describes gapped magnitude fluctuations. Solid line describes gapless phase fluctuations.

Finite-size effects are not expected to be large for small n, where Δ_n depend mostly on short-range correlations. We notice a striking difference between even and odd recurrents, which seem to follow *two* linearly increasing slopes. This even-odd effect of the recurrents is an indicator (not a proof) of a gaplike structure.[51]

Motivated by the field theoretical calculation, we use the trial function,

$$\tilde{G}''_{T=0} \propto G''_{\mathrm{RGP}}(\omega)\exp(-\omega^2/\Omega_0^2), \tag{87}$$

where m—the mass gap and Ω_0—the high-frequency falloff are variational parameters. We use Eq. (40) to determine the trial recurrents. The variational parameters are then determined by a least-squares fit between the exact and trial recurrents.

Thus we obtain,

$$\Omega_0 \to 8.6J,$$

$$m \to 10.9J. \tag{88}$$

The mass gap appears to be similar to the high-frequency Gaussian falloff of the conductivity at high temperatures, as given by the linear slope of the recurrents, Eq. (71).

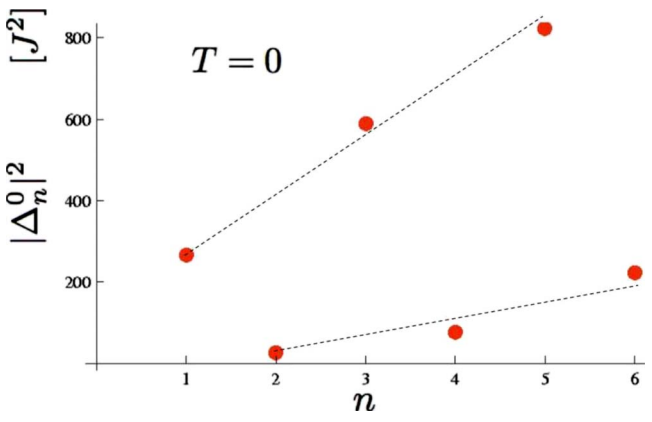

FIG. 7. (Color online) The recurrents of $G''_{T=0}(\omega)$ at zero temperature. Dashed line emphasizes the different behavior of even and odd recurrents, which is related to the gap structure in Fig. 8.

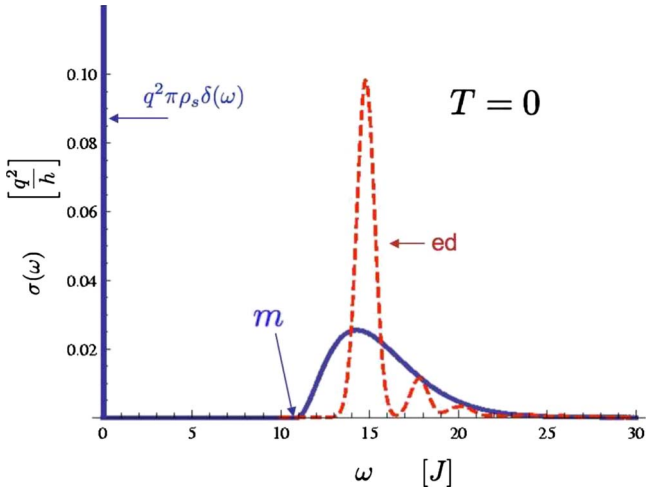

FIG. 8. (Color online) Zero-temperature dynamical conductivity of HCB. The Higgs mass gap m is depicted. Solid line (blue online) is determined by variationally fitting the recurrents to those in Fig. 7. Dashed line (red online) is computed by exact diagonalization of a 20-site cluster, with δ-function broadening of $0.5J$.

The resulting dynamical conductivity is depicted in Fig. 8. The figure also includes, for comparison, the results of exact diagonalization on a 16-site cluster, as given, for $\omega>0$ by

$$\tilde{G}''_{ed}(\omega) = \pi\sum_m |\langle 0|J_x|m\rangle|^2\delta(\omega + E_0 - E_m). \tag{89}$$

The oscillations in $\tilde{G}''_{ed}$ are artifacts of finite-size gaps in the spectrum. We see that the two curves agree on the position of the central peak and the total spectral weight.

A test of these calculations is provided by the zero-temperature f-sum rule is

$$\frac{h}{q^2}\int_{0+}\frac{d\omega}{\pi}\frac{G''_{T=0}(\omega)}{\omega} = \langle -K_x\rangle - \rho_s. \tag{90}$$

The left-hand side for the variational and exact diagonalization results yields

$$\frac{h}{q^2}\int_{0+}\frac{d\omega}{\pi}\frac{\tilde{G}''_{T=0}(\omega)}{\omega} = \begin{cases} 0.0148J & \text{Variational} \\ 0.0164J & \text{ED} \end{cases}. \tag{91}$$

The sum rules are comparable in magnitude to values obtained by QMC (Ref. 6) for the zero-temperature kinetic energy and superfluid stiffness,

$$\langle -K_x\rangle = 1.09765(4)J,$$

$$\rho_s = 1.078(1)J,$$

$$\rightsquigarrow \langle -K_x\rangle - \rho_s = 0.019(1)J. \tag{92}$$

We notice the very small spectral weight (2%) of the high-frequency peak at zero temperature, relative to the condensate weight. This weight is due to the quantum fluctuations of the ground state and to the nonconservation of the current operator in two dimensions. This weight can be ascribed to the magnitude oscillations mode.

Note. An important question is whether the mass gap survives corrections to Eq. (84). Within our variational approach, we tried to answer this question by allowing subgap spectral weight parameterized by a power-law tail such as

$$\tilde{G}''_{T=0} \propto \left[\frac{(|\omega|/m)^{\alpha}}{1+(|\omega|/m)^{\alpha}} \right] \exp(-\omega^2/\Omega_0^2). \tag{93}$$

The least-squares fit of the recurrents has found that α tends to increase indefinitely. This is consistent (although not being a proof) with having a true gap at $\omega=m$.

VIII. DISCUSSION

A. Bad metallicity

HCB at half filling exhibits *bad metal* characteristics, as demonstrated in Eq. (2) and in Fig. 1. In contrast to conventional metals and bosonic gases at high temperatures,[20–22] the resistivity of HCB rises approximately linearly, without a sign of saturation at $R \approx h/q^2$. Such behavior signals the breakdown of Boltzmann equation since the mean-free path becomes shorter than interparticle distance.[19]

We note that the fact that the resistivity reaches an asymptotically linear behavior is, in itself, not surprising for any system of lattice particles with a bounded bandwidth. Here we find that the linearity starts already at $2T_{\mathrm{BKT}}$, due to the relatively weak T^{-3} corrections. We do not have reasons to believe that the precise regime of linearity is universal with respect to changes in the model. We do expect however, that the conductivity reaches its asymptotic linearity at temperatures higher than the boson bandwidth, which is the only relevant energy scale in the model. This is very different than metallic superconductors, whose normal-state resistivity is governed by Fermi-liquid temperature scales which are generally much higher than their T_c.

A related quantity is the width of the low-frequency conductivity peak, which in metals is called the "Drude peak." Here, Eq. (2) shows that the low-frequency temperature-dependent peak in $\sigma(\omega)$ is governed mostly by the fluctuation-dissipation factor.[52] If one fits the width by Eq. (1) in the regime $T_{\mathrm{BKT}} < T \ll \bar{\Omega}$, one obtains

$$\left(\frac{1}{\tau}\right)^{\mathrm{eff}} = 2T. \tag{94}$$

We note however, that for our Hamiltonian (5), T_{BKT} is not much smaller than $\bar{\Omega}$. Therefore, separating the two frequency scales in $\sigma(T,\omega)$ is difficult. However, the ratio of the two scales can be made larger by additional interactions.

The HCB model relates the asymptotic resistivity slope to the zero-temperature superfluid stiffness,

$$\frac{dR^{\infty}}{dT} = 0.245 \frac{R_Q}{\rho_s}. \tag{95}$$

In a three-dimensional system of weakly coupled layers, the transition temperature T_c is shifted from T_{BKT} by a factor given by Eq. (13).[14,32] Above T_c the density of free vortices rises rapidly, which causes the rise in $R(T)$, as shown in Fig. 1. We can operationally define a nominal *critical normal-state resistivity* R_c by

$$R_c \equiv \frac{dR^{\infty}}{dT} T_c. \tag{96}$$

Thus, a HCB version of Homes law is obtained

$$\rho_s(0) = 0.245 \frac{R_Q}{R_c} T_c. \tag{97}$$

B. Cuprate conductivity

A large linear in T resistivity[23] and optical relaxation rate[53,54] are widely observed in clean samples, especially near optimal doping. It has been shown[55] that the linear resistivity is not consistent with a proximity to a quantum critical point.

It is plausible, therefore, that the bad metal characteristics of the normal phase of cuprates may be described by lattice bosons in their resistive state. Support to this viewpoint is given by Uemura's empirical scaling law $T_c \propto \rho_s^{ab}(T=0)$ (Ref. 12) and the observation of a superfluid density jump in ultrathin underdoped cuprate films.[56] These are consistent with the behavior of a bosonic superfluid, captured by an effective XY model. In underdoped cuprates, additional evidence exists that the hole pair bosons survive above T_c, up to the pseudogap temperature scale[57,58] $T^* > T_c$. Thus there have been several theoretical approaches[14,59–62] to the superconducting properties of cuprates based on lattice bosons of charge $q=2e$.

We note, however, that above the pseudogap temperature and frequency scale T^*, hole pairs completely disintegrate. Thus, *above* T^*, the HCB model cannot be used to obtain the temperature and frequency dependence correctly.

Homes *et al.*[24] have pointed out that the superfluid stiffness is generally proportional, with a seemingly universal constant, to the product of "critical conductivity" $\sigma_c^{3\mathrm{D}}$ and T_c. The critical conductivity $\sigma_c^{3\mathrm{D}}$ was experimentally defined by extrapolating $\sigma(\omega, T_c)$ to zero frequency. This empirically universal scaling was interpreted as a sign of "dirty superconductors," where T_c is determined by the disorder driven scattering rate.[63]

Here we promote a different viewpoint, which maintains that Homes law can also be obtained in a *disorder free* model. The necessary ingredients are strong scattering effects, as described by hard core bosons above T_{BKT}.

To relate the experimental data of cuprates to the HCB model, we first translate the 3D critical conductivity to a two-dimensional critical conductivity,

$$\sigma_c = a_c \sigma_c^{3\mathrm{D}}, \tag{98}$$

where $a_c \approx 1.5$ nm is the interplane distance.

The zero-temperature boson superfluid stiffness can be deduced from the in-plane London penetration depth,

$$\rho_s = a_c \rho_s^{3\mathrm{D}} = \frac{\hbar^2 c^2}{16\pi e^2} \frac{a_c}{\lambda_{ab}^2}, \tag{99}$$

where c is the speed of light or the optical plasma frequency ω_{ps},

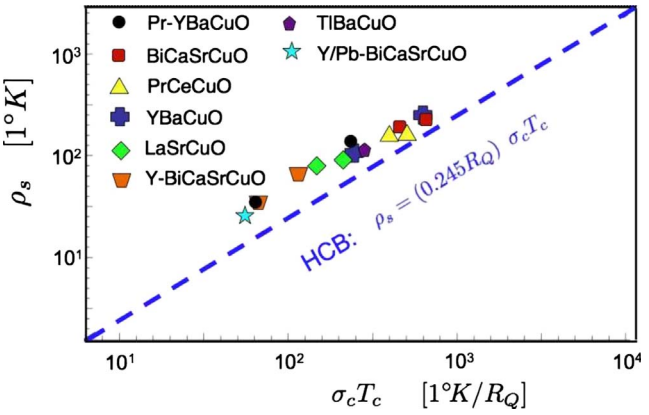

FIG. 9. (Color online) Comparison of Homes law of HCB and cuprate superconductors. HCB calculation is depicted by the dashed line (blue online). Cuprate data, compiled from Refs. 24 and 63, describe the two-dimensional critical conductivity σ_c, as measured by optical conductivity exprapolated to zero frequency, at the transition temperature T_c. ρ_s values are compiled from measured plasma frequencies by Eq. (100). R_Q=6453 Ω is the boson quantum of resistance. Different data points of the same symbol correspond to different doping concentrations of the same compound.

$$\rho_s = \frac{\hbar^2}{16\pi e^2} a_c \omega_p^2. \tag{100}$$

In Fig. 9 we plot the data reported in Refs. 24 and 63 by translating it into the two-dimensional quantities. We find, quite remarkably, that the slope of Eq. (97) lies quite close to the experimental data. We emphasize that the proportionality constant in Eq. (97) is not expected to be universal. *A priori*, one might expect it to vary with additional interactions and the filling. If the agreement with cuprates' data is not fortuitous, it would imply that this constant might not be sensitive to moderate variations of H.

At very low temperatures, we find that there is a signature of the quantum fluctuations of the order parameter in the optical conductivity at high frequencies. These are magnitude fluctuations characterized by a Higgs mass gap at frequency

$$m \approx 10\rho_s. \tag{101}$$

It is interesting to mention that such a massive magnitude mode, given by the relativistic Gross-Pitaevskii action, appears in the superfluid phase of the strongly interacting Bose Hubbard model at integer filling. It has been associated with the "oscillating superfluidity" experiments of cold atoms in an optical lattice.[25–27]

While a clear signature of such a peak in cuprates has not been identified, we speculate that it might be related to the ubiquitous *mid infrared peak* which has been detected in several compounds at low temperatures.[28] We caution, however, that at these high frequencies, additional fermionic excitations become increasingly important.

In summary, we conclude that some of the "normal-state" phenomenology of cuprates in the pseudogap regime, and perhaps also other unconventional superconductors, may be described by lattice bosons. We do not have an explanation for the observed T-linear resistivity of cuprates well above the pairing temperature T^*. This would require solving for the conductivity of a coupled boson-fermion Hamiltonian, which is beyond the scope of this work.

In addition, Eq. (5) oversimplifies cuprates by omitting potentially important interactions such as long-range Coulomb interactions, interlayer coupling, disorder and inhomogeneities, and of course the HCB conductivity away from half filling. Clearly, these effects need to be accounted for in future work.

ACKNOWLEDGMENTS

We thank Dan Arovas, Yosi Avron, Dimitri Basov, George Batrouni, Christopher Homes, David Huse, Peter Jung, Steve Kivelson, Daniel Podolsky, and Efrat Shimshoni for useful discussions. We acknowledges support from Israel Science Foundation and US—Israel Binational Science Foundation. A.A. is grateful for Aspen Center for Physics which inspired some of the ideas in this paper. N.L. acknowledges the financial support of the Israel Clore foundation.

APPENDIX A: ORTHOGONAL POLYNOMIALS AND RECURRENTS

Iterative use of the matrix inversion formula for $G_n(z)$,

$$G_n(z) = \mu_0 (z - L)^{-1}_{n,0} \tag{A1}$$

with L defined as in Eq. (37) yields for $z \to \omega + i\epsilon$

$$G_n''(\omega) = P_n(\omega) G_0(\omega), \tag{A2}$$

where $P_n(\omega)$ is a polynomial that depends on the $|\Delta_m|^2$'s for $m \le n$ and is given by

$$P_n(\omega) = \prod_{k=1}^{n} |\Delta_k|^{-1} \det(\omega - L)_{n-1}. \tag{A3}$$

In the above, $(z-L)_{n-1}$ is the upper left $n \times n$ submatrix of $(z-L)$.

The determinants $\det(z-L)_{n-1}$ obey the recursion relation

$$\det(z-L)_{n+1} = z \det(z-L)_n - |\Delta_n|^2 \det(z-L)_{n-1}. \tag{A4}$$

Equation (A4) is a recursion relation for orthogonal polynomials. The polynomials $P_n(\omega)$ defined in Eq. (A3) are therefore orthogonal polynomials under the scalar product defined by

$$\int_{-\infty}^{\infty} d\omega G_0(\omega) P_n(\omega) P_m(\omega) = \delta_{nm}. \tag{A5}$$

The complexity of computation of $C_n(\beta)$ and $P_n(\omega)$ depends on obtaining all the low $\Delta_m, m \le n$. Therefore, the expansion [Eq. (51)] would be useful if it could be truncated at finite n, provided that the coefficients $C_n(\beta)$ decay rapidly enough with n.

APPENDIX B: LINEAR RECURRENTS AND THE GAUSSIAN SPECTRAL DENSITY

Let us consider a sequence of recurrents $|\Delta_n|^2$ given by

$$|\Delta_n|^2 = \tfrac{1}{2} n\Omega^2 \quad n = 1,2,\ldots \tag{B1}$$

The continued fraction representation can be solved using the following map. Consider the dimensionless position operator $\hat{x}$ represented by raising and lowering operators of the one-dimensional harmonic oscillator

$$x = \frac{1}{\sqrt{2}}(a^\dagger + a). \tag{B2}$$

Since we have $\langle n+1|\hat{x}|n\rangle = \sqrt{(n+1)/2}$, the function $G_n(z)$ of Eq. (50) is equivalent to

$$G_n(z) = \mu_0 \langle n| \frac{1}{z - \Omega\hat{x}} |0\rangle. \tag{B3}$$

Using the x representation for the ground state of the harmonic oscillator we have

$$G_0(\omega)/\mu_0 = \int_{-\infty}^{\infty} dx \frac{1}{\omega + i\epsilon - \Omega x} \frac{e^{-x^2}}{\sqrt{\pi}}$$
$$= -i\sqrt{\frac{\pi}{\Omega}} e^{-\omega^2/\Omega^2} \left(1 + \frac{2i}{\pi} \int_0^{\omega^2/\Omega^2} e^{t^2} dt\right). \tag{B4}$$

Likewise, for higher values of n we have

$$-\mathrm{Im}\, G_n(\omega)/\mu_0 = \mathrm{Im} \int_{-\infty}^{\infty} dx \frac{N_n H_n(x)}{\omega + i\epsilon - \Omega x} \frac{e^{-x^2}}{\sqrt{\pi}}$$
$$= \frac{\sqrt{\pi}}{2} e^{-\omega^2/\Omega^2} N_n H_n(\omega/\Omega), \tag{B5}$$

where $N_n = 1/\sqrt{2^n n!}$.

[1] J. M. Ziman, *Electrons and Phonons* (Oxford University Press, New York, 1960).
[2] G. D. Mahan, *Many-Particle Physics* (Plenum, New York, 1981).
[3] E. Loh, Jr., D. J. Scalapino, and P. M. Grant, Phys. Rev. B **31**, 4712 (1985).
[4] H. Q. Ding and M. S. Makivić, Phys. Rev. B **42**, 6827 (1990).
[5] H. Q. Ding, Phys. Rev. B **45**, 230 (1992).
[6] A. W. Sandvik and C. J. Hamer, Phys. Rev. B **60**, 6588 (1999).
[7] K. Bernardet, G. G. Batrouni, J.-L. Meunier, G. Schmid, M. Troyer, and A. Dorneich, Phys. Rev. B **65**, 104519 (2002).
[8] N. H. Lindner, A. Auerbach, and D. P. Arovas, Phys. Rev. Lett. **102**, 070403 (2009).
[9] A. Auerbach and N. Lindner, arXiv:0902.2822 (unpublished).
[10] L. Pitaevskii and S. Stringari, *Bose Einstein Condensation* (Oxford University Press, New York, 2003).
[11] D. Jaksch and P. Zoller, Ann. Phys. **315**, 52 (2005).
[12] Y. J. Uemura, G. M. Luke, B. J. Sternlieb, J. H. Brewer, J. F. Carolan, W. N. Hardy, R. Kadono, J. R. Kempton, R. F. Kiefl, S. R. Kreitzman, P. Mulhern, T. M. Riseman, D. Ll. Williams, B. X. Yang, S. Uchida, H. Takagi, J. Gopalakrishnan, A. W. Sleight, M. A. Subramanian, C. L. Chien, M. Z. Cieplak, Gang Xiao, V. Y. Lee, B. W. Statt, C. E. Stronach, W. J. Kossler, and X. H. Yu, Phys. Rev. Lett. **62**, 2317 (1989).
[13] V. J. Emery and S. A. Kivelson, Nature (London) **374**, 434 (1995).
[14] A. Mihlin and A. Auerbach, Phys. Rev. B **80**, 134521 (2009).
[15] A. van Oudenaarden and J. E. Mooij, Phys. Rev. Lett. **76**, 4947 (1996).
[16] E. Altman and A. Auerbach, Phys. Rev. Lett. **81**, 4484 (1998).
[17] M. P. A. Fisher, P. B. Weichman, G. Grinstein, and D. S. Fisher, Phys. Rev. B **40**, 546 (1989).
[18] B. I. Halperin and D. Nelson, J. Low Temp. Phys. **36**, 599 (1979).
[19] V. J. Emery and S. A. Kivelson, Phys. Rev. Lett. **74**, 3253 (1995).
[20] A. F. Ioffe and A. R. Regel, Prog. Semicond. **4**, 237 (1960).
[21] A. Auerbach and P. B. Allen, Phys. Rev. B **29**, 2884 (1984).
[22] P. B. Allen, Comments Condens. Matter Phys. **15**, 327 (1992).
[23] N. P. Ong, in *Physical Properties of High Temperature Superconductotrs*, edited by D. L. Ginsberg (World Scientific, Singapore, 1990).
[24] C. C. Homes, S. V. Dordevic, M. Strongin, D. A. Bonn, Ruixing Liang, W. N. Hardy, Seiki Komiya, Yoichi Ando, G. Yu, N. Kaneko, X. Zhao, M. Greven, D. N. Basov, and T. Timusk, Nature (London) **430**, 539 (2004); C. C. Homes, Phys. Rev. B **80**, 180509(R) (2009).
[25] C. Orzel, A. K. Tuchman, M. L. Fenselau, M. Yasuda, and M. A. Kasevich, Science **291**, 2386 (2001).
[26] M. Greiner, O. Mandel, T. Esslinger, T. W. Hansch, and I. Bloch, Nature (London) **415**, 39 (2002).
[27] E. Altman and A. Auerbach, Phys. Rev. Lett. **89**, 250404 (2002).
[28] K. Holczer, L. Forro, L. Mihaly, and G. Gruner, Phys. Rev. Lett. **67**, 152 (1991); M. C. Nuss, P. M. Mankiewich, M. L. OMalley, E. H. Westerwick, and P. B. Littlewood, *ibid.* **66**, 3305 (1991); D. B. Romero, C. D. Porter, D. B. Tanner, L. Forro, D. Mandrus, L. Mihaly, G. L. Carr, and G. P. Williams, *ibid.* **68**, 1590 (1992).
[29] J. M. Kosterlitz and D. J. Thouless, J. Phys. C **5**, L124 (1972).
[30] J. M. Kosterlitz and D. J. Thouless, J. Phys. C **6**, 1181 (1973).
[31] V. L. Berezinskii, Sov. Phys. JETP **34**, 610 (1972).
[32] S. Hikami and T. Tsuneto, Prog. Theor. Phys. **63**, 387 (1980).
[33] E. W. Carlson, S. A. Kivelson, V. J. Emery, and E. Manousakis, Phys. Rev. Lett. **83**, 612 (1999).
[34] A. L. Fetter, Ann. Phys. (N.Y.) **60**, 464 (1970).
[35] R. Micnas, S. Robaszkiewicz, and T. Kostyrko, Phys. Rev. B **52**, 6863 (1995).
[36] D. J. Scalapino, S. R. White, and S. Zhang, Phys. Rev. B **47**, 7995 (1993).
[37] D. D. Betts, in *Phase Transition and Critical Phenomena*, edited by C. Domb and M. C. Green (Academic, New York, 1974), Vol. 6.

[38] H. Mori, Prog. Theor. Phys. **34**, 399 (1965).
[39] M. H. Lee, Phys. Rev. B **26**, 2547 (1982).
[40] *Handbook of Mathematical Functions*, edited by M. Abramowitz and I. A. Stegun (Dover, New York, 1969).
[41] In one dimension $\mathcal{L}J_x=0$ and all moments vanish.
[42] Dan Arovas (private communication).
[43] J. Rogiers, T. Lookman, D. D. Betts, and C. J. Elliot, Can. J. Phys. **56**, 409 (1979).
[44] S. Mukerjee, V. Oganesyan, and D. Huse, Phys. Rev. B **73**, 035113 (2006).
[45] David Huse (private communication).
[46] V. Ambegaokar, B. I. Halperin, D. R. Nelson, and E. D. Siggia, Phys. Rev. Lett. **40**, 783 (1978).
[47] V. Ambegaokar, B. I. Halperin, D. R. Nelson, and E. D. Siggia, Phys. Rev. B **21**, 1806 (1980).
[48] M. P. A. Fisher and D. H. Lee, Phys. Rev. B **39**, 2756 (1989).
[49] K. Damle and S. Sachdev, Phys. Rev. B **56**, 8714 (1997).
[50] M.-C. Cha, M. P. A. Fisher, S. M. Girvin, M. Wallin, and A. P. Young, Phys. Rev. B **44**, 6883 (1991).
[51] V. S. Viswanath, S. Zhang, J. Stolze, and G. Muller, Phys. Rev. B **49**, 9702 (1994).
[52] Similar factorization of the dynamical conductivity into a fluctuation-dissipation factor times a broader, weakly temperature-independent function was found for the t-J model by J. Jaklic and P. Prelovsek, Phys. Rev. Lett. **75**, 1340 (1995); and for the Kondo model by V. J. Emery and S. Kivelson, Phys. Rev. B **46**, 10812 (1992).
[53] A. V. Puchkov, D. N. Basov, and T. Timusk, J. Phys.: Condens. Matter **8**, 10049 (1996).
[54] D. N. Basov. and T. Timusk, Rev. Mod. Phys. **77**, 721 (2005).
[55] P. Phillips and C. Chamon, Phys. Rev. Lett. **95**, 107002 (2005).
[56] M. B. Salamon, J. Shi, N. Overend, and M. A. Howson, Phys. Rev. B **47**, 5520 (1993); S. Kamal, D. A. Bonn, N. Goldenfeld, P. J. Hirschfeld, R. Liang, W. N. Hardy, Phys. Rev. Lett. **73**, 1845 (1994); I. Hetel, T. R. Lemberger, and M. Randeria, Nat. Phys. **3**, 700 (2007).
[57] S. Hufner, M. A. Hossain, A. Damascelli, and G. A. Sawatzky, Rep. Prog. Phys. **71**, 062501 (2008).
[58] A. N. Pasupathy, A. Pushp, K. K. Gomes, C. V. Parker, J. Wen, Z. Xu, G. Gu, S. Ono, Y. Ando, and A. Yazdani, Science **320**, 196 (2008).
[59] T. Kostyrko and J. Ranninger, Phys. Rev. B **54**, 13105 (1996).
[60] A. Paramekanti, M. Randeria, T. V. Ramakrishnan, and S. S. Mandal, Phys. Rev. B **62**, 6786 (2000); H. J. Kwon, A. T. Dorsey, and P. J. Hirschfeld, Phys. Rev. Lett. **86**, 3875 (2001).
[61] E. Altman and A. Auerbach, Phys. Rev. B **65**, 104508 (2002).
[62] M. Franz and A. P. Iyengar, Phys. Rev. Lett. **96**, 047007 (2006); I. F. Herbut and M. J. Case, Phys. Rev. B **70**, 094516 (2004).
[63] C. C. Homes, S. V. Dordevic, T. Valla, and M. Strongin, Phys. Rev. B **72**, 134517 (2005).